European Journal of Mechanics / A Solids 69 (2018) 231–237

Contents lists available at ScienceDirect

European Journal of Mechanics / A Solids

journal homepage: www.elsevier.com/locate/ejmsol

Dynamics of a beam with both axial moving and spinning motion: An example of bi-gyroscopic continua

Xiao-Dong Yang[a,*], Ji-Hou Yang[a], Ying-Jing Qian[a], Wei Zhang[a], Roderick V.N. Melnik[b]

[a] Beijing Key Laboratory of Nonlinear Vibrations and Strength of Mechanical Engineering, College of Mechanical Engineering, Beijing University of Technology, Beijing 100124, China

[b] The MS2Discovery Interdisciplinary Research Institute, M2NeT Laboratory, Wilfrid Laurier University, 75 University Avenue West, Waterloo, ON, N2L 3C5, Canada

ARTICLE INFO

Keywords:
Bi-gyroscopic system
Axially moving and spinning material
Bifurcation

ABSTRACT

Classical gyroscopic continua include axially moving materials and spinning structures. The gyroscopic effect of the axially moving material is pronounced via the gyroscopic coupling among the basis functions in the same motional direction. On the other hand, the gyroscopic coupling of the spinning structure acts in the two different directions of motion. In this paper, we study the dynamics of a beam with both axial moving motion and spinning motion as a prototype of bi-gyroscopic continua. The influence of bi-gyroscopic effects on the natural frequencies, modes, and stability is investigated by an analytical method applied to the discretized equations of the axially moving and spinning beam. Distinct bifurcation series of the eigenvalues and corresponding physical interpretations are discussed by numerical display of the modal motions. The complex modes describing both whirling motions and traveling waves are investigated in detail for such bi-gyroscopic system. New interesting phenomena have been analyzed numerically and important conclusions have been drawn for such bi-gyroscopic system.

1. Introduction

From a broader perspective, mechanical structures that can vibrate about a state of mean rotation are classified as gyroscopic dynamic systems. The gyroscopic effect comes from the Coriolis force measured on the rotating frame. Spinning flexible structure is a straightforward example of the gyroscopic continua. Another example is the axially moving material, for which the rotating frame is observed on the slope variation of the overall contour.

In the case of spinning structure as presented in Fig. 1(a), the spinning velocity is $\overline{\Omega}$ and the transverse displacement in Z direction is W, and the corresponding velocity is $\partial W/\partial T$. The Coriolis force on a small element caused by the Z directional motion is $2\overline{\Omega}\,(\partial W/\partial T)$, along the Y direction. On the other hand, if the displacement and velocity in Y direction is measured, the Coriolis force in Z direction will be generated. Hence, the Coriolis force of the spinning structure makes every element of the continuum vibrating in the YZ plane, showing the elliptic whirling motions. The gyroscopic coupling between the two transverse directions is the feature of the spinning bodies.

In the case of axially moving structure as presented in Fig. 1(b), the axially moving velocity is U and the transverse displacement in Z direction is W. An arbitrary element of the flexible structure, excluding the supporting ends, involves a rotating velocity $\partial^2 W/\partial X\partial T$. The Coriolis force is then $2U\,(\partial^2 W/\partial X\partial T)$ along the transverse Z direction. Similarly, the motion in the Y direction will cause Coriolis force in the same direction. Hence, contrary to the spinning structures, the two transverse directional motions are not coupled gyroscopically through the Coriolis force for the axial moving structures. Actually, the gyroscopic coupling acts on different basis functions along the same transverse direction.

From the above discussions, two types of gyroscopic continua emerge: spinning structures and axially moving structures. The gyroscopic effects present different phenomena in the two types of gyroscopic continua: (a) the two transverse directions of the spinning structure are gyroscopically coupled by the Coriolis force, which leads to whirling motions in the YZ plane, and (b) the basis functions on the same transverse direction of the axially moving material are gyroscopically coupled by the Coriolis force, which leads to travelling waves in XZ and XY plane, independently.

The presence of the gyroscopic terms in the governing equations of the gyroscopic continua limits analytical results, but enriches the dynamical behaviors dramatically. In the study of spinning well balanced axisymmetric structures, like spinning disks (Fang et al., 2014; Genta, 2005), spinning rings (Cooley and Parker, 2014; Genta and Silvagni,

* Corresponding author.
E-mail address: jxdyang@163.com (X.-D. Yang).

https://doi.org/10.1016/j.euromechsol.2018.01.006
Received 21 May 2017; Received in revised form 19 January 2018; Accepted 22 January 2018

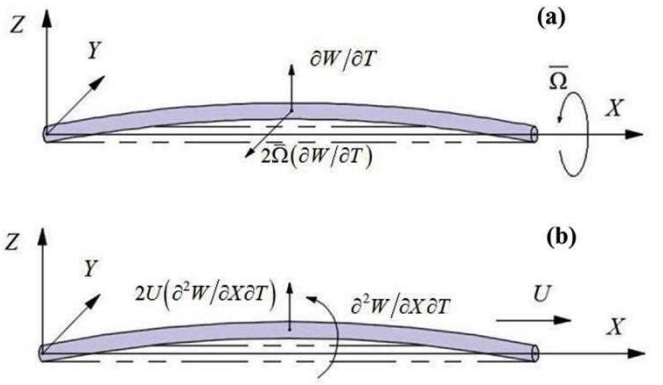

Fig. 1. The two types of gyroscopic continua. (a) Spinning structure; (b) Axially moving structure.

2013; Kim and Chung, 2002), spinning beam (Wu et al., 2014) and spinning disk-spindle systems (Parker and Sathe, 1999a, b), it is found that the natural frequency of each mode for the stationary structure branches into two because the spinning motion couples the two transverse directions and transfers the two isolated equal frequencies into distinct ones. In general, these branches represent the natural frequencies for the forward and backward whirling motions. In the study of axially moving materials, like pipes conveying fluid (Païdoussis, 1998; Yu et al., 2014), axially moving strings (Chen, 2005; Parker, 1998; Wickert and Mote, 1989) and axially moving beams (Öz and Pakdemirli, 1999; Parker, 1998), it is concluded that the natural frequencies will decrease with the increasing axial velocity until the divergence occurs, beyond which the system loses its stability. However, due to the gyroscopic terms, the axially moving structure may regain stability and, with further increase of velocity, loses stability by flutter. Due to the gyroscopic effect, the 'travelling waves' of the axially moving material during modal motions have been studied, which are different from the 'standing waves' of the static structure (Yang et al., 2016). From the Galerkin discretized point of view, the 'standing waves' are maintained because the basis functions (sine functions for the both end supported case) are exactly the solutions of the static structure and 'travelling waves' are caused due to the fact that the solutions are composed of coupled basis functions with phase differences.

The differences of the spinning structure and axially moving material as mono-gyroscopic continua have been listed in Table 1. The gyroscopic dynamics found in the two types of gyroscopic continua are different for both the coupling style and the vibration phenomena. One question then arises from the comparison: what dynamics will arise if the structure undergoing both spinning and axial motion? In the present study, we answer this question by proposing a novel idea of the bi-gyroscopic effect: a gyroscopic effect from both spinning and axially moving motion, which belong to two different types of gyroscopic couplings.

In the engineering field, the structures with both spinning and axial motion are used, among other applications, as a component in drilling machines (Arvajeh and Ismail, 2006; Rincon and Ulsoy, 1995) and drilling oil pipes (Pei et al., 2013; Zhang and Miska, 2005). In the

Table 1
Comparison of the two types of gyroscopic continua.

	Modal motions	Coupling	Gyroscopic features
Spinning structure	Whirling	Two transverse directions coupled	One frequency braches into two.
Axially moving structure	Travelling wave	Basis functions in the same direction coupled	Two stable regions exist; Bifurcate from stability to divergence, and then from restability to flutter.

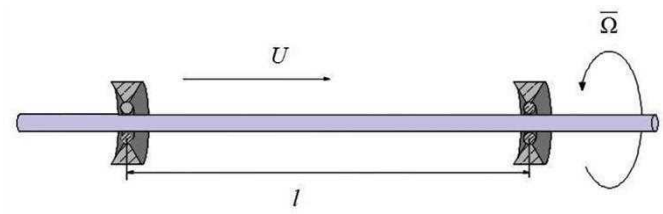

Fig. 2. Diagram of beam undergoing both spinning and axial moving motion.

available dynamical studies of the drilling slender continua, the axial motion has been usually neglected. On the other hand, from the theoretical point of view, a combination of spinning and axial motion may lead to rich dynamics of the gyroscopic system. In this paper, a prototype of bi-gyroscopic continua is investigated based on the beam model undergoing both spinning and axial motion. The features of the bi-gyroscopic couplings and modal motions are studied and discussed. The bifurcation series of the dynamics based on the eigenproblem is analyzed in detail, which may provide a foundation for further investigations on structures with bi-gyroscopic couplings.

2. System model

A circular flexible beam simply supported by two joints with distance l, is undergoing both spinning motion with constant velocity $\overline{\Omega}$ and axial moving motion with constant speed U, as shown in Fig. 2. The stiffness, cross section area and density of beam material is EI, A and ρ, respectively. To derive the displacements of the flexible beam, two sets of rotating reference coordinates are used: $OXYZ$ is a spinning reference frame with spinning velocity $\overline{\Omega}$ along X axis; $PX_1Y_1Z_1$ is reference frame with both spinning and axial moving motion. Without the spinning velocity, the two reference frames recover the Euler and Lagrange descriptions of the axially moving material, respectively. The deflections of an arbitrary moving beam element can be observed in the $PX_1Y_1Z_1$ frame. However, the final visual displacements of the axis line of the beam are measured in the rotating frame $OXYZ$ (see Fig. 3).

The transformation relations of the two rotating references are

$$X_1 = X + UT, \quad Y_1 = Y, \quad Z_1 = Z. \tag{1}$$

If the transverse displacements V and W of an arbitrary point on the beam are defined on Y_1 and Z_1 direction, respectively, the position vector of such point P_1 in the $OXYZ$ frame is

$$\begin{aligned}\mathbf{OP}_1 &= (UT)\mathbf{i} + \mathbf{PP}_1 = (UT)\mathbf{i} + V(X_1, T)\mathbf{j} + W(X_1, T)\mathbf{k} \\ &= (UT)\mathbf{i} + V(X + UT, T)\mathbf{j} + W(X + UT, T)\mathbf{k}.\end{aligned} \tag{2}$$

Further, the velocity can be derived by the first derivative of (2) as

$$\mathbf{v} = U\mathbf{i} + \left(\frac{\partial V}{\partial T} + U\frac{\partial V}{\partial X} - \overline{\Omega}W\right)\mathbf{j} + \left(\frac{\partial W}{\partial T} + U\frac{\partial W}{\partial X} + \overline{\Omega}V\right)\mathbf{k}. \tag{3}$$

Then the kinetic energy and potential energy are, respectively,

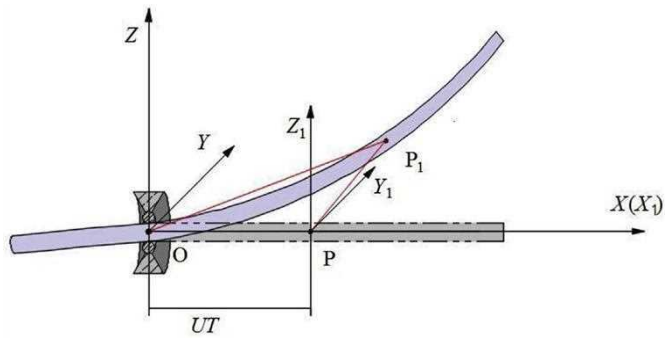

Fig. 3. Deformation of the structure.

$$T_k = \frac{1}{2}\rho A\int_0^l \left[U^2 + \left(\frac{\partial V}{\partial T} + U\frac{\partial V}{\partial X} - \overline{\Omega} W\right)^2 + \left(\frac{\partial W}{\partial T} + U\frac{\partial W}{\partial X} + \overline{\Omega} V\right)^2\right] dX, \tag{4}$$

$$U_p = \frac{1}{2}EI\int_0^l \left(\left(\frac{\partial^2 V}{\partial X^2}\right)^2 + \left(\frac{\partial^2 W}{\partial X^2}\right)^2\right) dX. \tag{5}$$

Applying the kinetic and potential energies of the system to Hamilton's principle and using the dimensionless variables and parameters yield the governing equations of motion along Y and Z directions,

$$\frac{\partial^2 v}{\partial t^2} + \frac{\partial^4 v}{\partial x^4} + u^2\frac{\partial^2 v}{\partial x^2} - \Omega^2 v + \overline{2u\frac{\partial^2 v}{\partial t\partial x}} - \underline{2\Omega\frac{\partial w}{\partial t}} - \underline{2u\Omega\frac{\partial w}{\partial x}} = 0, \tag{6}$$

$$\frac{\partial^2 w}{\partial t^2} + \frac{\partial^4 w}{\partial x^4} + u^2\frac{\partial^2 w}{\partial x^2} - \Omega^2 w + \overline{2u\frac{\partial^2 w}{\partial t\partial x}} + \underline{2\Omega\frac{\partial v}{\partial t}} + \underline{2u\Omega\frac{\partial v}{\partial x}} = 0, \tag{7}$$

and the boundary conditions

$$\begin{aligned} &x = 0: \quad v = w = 0, \quad \frac{\partial^2 v}{\partial x^2} = \frac{\partial^2 w}{\partial x^2} = 0,\\ &x = 1: \quad v = w = 0, \quad \frac{\partial^2 v}{\partial x^2} = \frac{\partial^2 w}{\partial x^2} = 0. \end{aligned} \tag{8}$$

In the above equations (6)–(8), the following dimensionless variables and parameters are used:

$$v = \frac{V}{l}, \quad w = \frac{W}{l}, \quad x = \frac{X}{l}, \quad t = T\sqrt{\frac{EI}{\rho A l^4}}, \quad \Omega = \overline{\Omega}\sqrt{\frac{\rho A l^4}{EI}}, \quad u = U\sqrt{\frac{\rho A l^2}{EI}}. \tag{9}$$

In (6) and (7), the terms related to the first derivative with respect to time t are gyroscopic terms. The underlined terms, proportional to spinning velocity, provide the coupling between the two directions since they appear in both equations. The over bar terms, proportional to axial moving velocity, provide the coupling among basis functions along the same direction. Interesting terms are those underlined with double lines. They are caused by a combined contribution of spinning and axial motion, leading to stiffness coupling between different directions and basis functions. Inspection of (6) and (7) also yields the conclusion that governing equations can be recovered to the pure axially moving case with $\Omega = 0$ and to the pure spinning case with $u = 0$.

3. Discretized system analysis

The discretized ordinary differential equations can be obtained by the Galerkin truncation method. The sine mode functions of the static beam are adopted as basis functions. It is known that the axially moving velocity leads to the couplings among the basis functions (Pellicano and Vestroni, 2000; Wickert and Mote, 1990). The coupling among the sine basis functions transfers the standing wave of the static beam into a traveling wave of the axially moving beam (Yang et al., 2016).

Substituting the following equations

$$\begin{aligned} v(x,t) &= \sum_{k=1}^{N} Q_k(t)\sin(k\pi x),\\ w(x,t) &= \sum_{n=1}^{N} P_n(t)\sin(n\pi x), \end{aligned} \tag{10}$$

and their derivatives into (6) and (7), and applying the Galerkin procedure yield

$$\begin{Bmatrix}\ddot{\mathbf{Q}}\\ \ddot{\mathbf{P}}\end{Bmatrix} + \begin{bmatrix}\mathbf{G}_1 & \mathbf{G}_2\\ -\mathbf{G}_2 & \mathbf{G}_1\end{bmatrix}\begin{Bmatrix}\dot{\mathbf{Q}}\\ \dot{\mathbf{P}}\end{Bmatrix} + \begin{bmatrix}\mathbf{K} & \mathbf{D}\\ -\mathbf{D} & \mathbf{K}\end{bmatrix}\begin{Bmatrix}\mathbf{Q}\\ \mathbf{P}\end{Bmatrix} = \begin{Bmatrix}0\\ 0\end{Bmatrix}, \tag{11}$$

where the elements in vectors $\mathbf{Q} = [Q_1, Q_2, \ldots, Q_N]^{\mathrm{T}}$, $\mathbf{P} = [P_1, P_2, \ldots, P_N]^{\mathrm{T}}$ are generalized coordinates, and the elements in the diagonal stiffness matrix $\mathbf{K}$, coupling stiffness matrix $\mathbf{D}$, same direction coupling gyroscopic matrix $\mathbf{G}_1$ and different direction coupling gyroscopic matrix $\mathbf{G}_2$ are, respectively,

$$\begin{aligned} (\mathbf{K})_{nk} &= \delta_{nk}[(n\pi)^4 - u^2(n\pi)^2 - \Omega^2]\\ (\mathbf{D})_{nk} &= \begin{cases} -\frac{8nk}{(k-n)(k+n)}u\Omega, & n+k \text{ is odd}\\ 0 & n+k \text{ is even}\end{cases}\\ (\mathbf{G}_1)_{nk} &= \begin{cases} -\frac{8nk}{(k-n)(k+n)}u, & n+k \text{ is odd}\\ 0, & n+k \text{ is even}\end{cases}\\ (\mathbf{G}_2)_{nk} &= -2\mathbf{I}\Omega. \end{aligned} \tag{12}$$

Clearly, there are two types of gyroscopic effects due to the matrices $\mathbf{G}_1$ dependent on u and $\mathbf{G}_2$ dependent on Ω. Those coupling matrices play key roles in the determining of dynamic characters of such a bi-gyroscopic system. The frequencies and corresponding complex modes of the bi-gyroscopic system can be investigated by the eigenvalue problem of (11).

The eigenvectors describe the contour of the beam with both axial and spinning motion during modal vibrations. We will determine the following characteristics of eigenvectors for this bi-gyroscopic system. The eigenvector corresponding to any eigenvalue can be denoted by a column of $2N$ elements, which can be written as $[\mathbf{V}_y, \mathbf{V}_z]^{\mathrm{T}}$. The upper N elements are corresponding to the vibration along y direction, and the lower N elements are corresponding to the vibration along z direction. Because of gyroscopic coupling between the two directions via $\mathbf{G}_2$, an arbitrary segment of the beam during modal motion undergoes an elliptic trajectory in the cross-sectional plane. When the deflection approaches maximum in one direction, the velocity in the other direction reaches its maximum. From a vibrational point of view, there exists a $\pi/2$ phase difference between the two directions. Correspondingly, the relation between the two parts in the same eigenvector is

$$\mathbf{V}_z = i\mathbf{V}_y. \tag{13}$$

In the same direction, y or z direction, the generalized coordinates of the basis functions are gyroscopically coupled via $\mathbf{G}_1$. The gyroscopic characteristics of such couplings have been discussed (Yang et al., 2016). It has been found that there always exists a $\pi/2$ phase difference between any of the two adjacent general coordinates during modal motions, that is,

$$v_2 = a_2\dot{v}_1, \quad v_3 = a_3 v_1, \quad v_4 = a_4\dot{v}_1, \quad v_5 = a_5 v_1, \quad \ldots \tag{14}$$

where the elements of $\mathbf{V}_z$ can be written in the following form:

$$\mathbf{V}_z = [1 \quad \mathrm{i}\omega a_2 \quad a_3 \quad \mathrm{i}\omega a_4 \quad a_5 \quad \cdots]^{\mathrm{T}}. \tag{15}$$

The real-value and imaginary-value elements are alternatively arranged in the eigenvector (15). Hence, during the modal motions, the displacements of the odd order coordinates are proportional to the displacement of the first order, and the displacements of the even order coordinates are proportional to the velocity (indicated by i) of the first order.

Using (10), (13) and (14), the final expression for the complex modes can be expressed as

$$\begin{aligned} V(x) &= A[\sin(\pi x) + \mathrm{i}\omega a_2\sin(2\pi x) + \sin(3\pi x) + \mathrm{i}\omega a_4\sin(4\pi x) + a_5\sin(5\pi x) + \cdots],\\ W(x) &= \mathrm{i}A[\sin(\pi x) + \mathrm{i}\omega a_2\sin(2\pi x) + \sin(3\pi x) + \mathrm{i}\omega a_4\sin(4\pi x) + a_5\sin(5\pi x) + \cdots]. \end{aligned} \tag{16}$$

Further inspection of (11) also confirms that the combination of the two motions not only provides two gyroscopic couplings but also stiffness coupling via matrix $\mathbf{D}$. It is proportional to the product of both axial and spinning motion velocity. Unloading either motion will lead to the vanishing of such stiffness coupling. This is a unique feature of such a bi-gyroscopic system.

In this study, the 4-term discretized system ($N = 4$) is used to show the varying rules of the frequencies and modes with different velocity

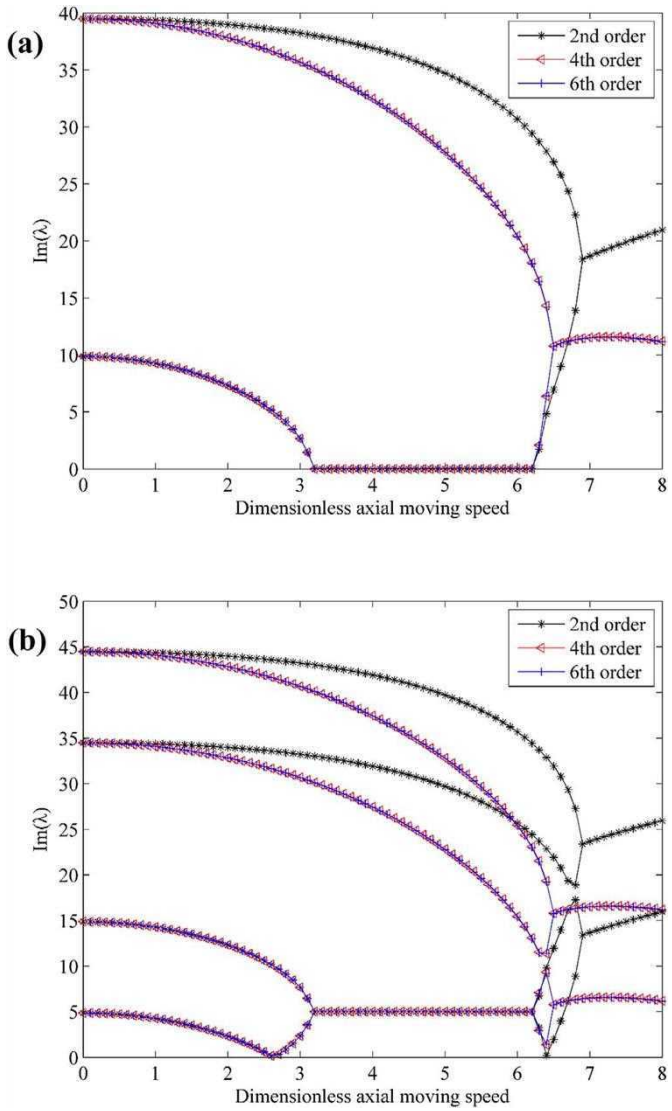

Fig. 4. Convergence of Galerkin truncation. (a) Spinning velocity $\Omega = 0$; (b) Spinning velocity $\Omega = 5$.

parameters. It has been verified that lower order truncation is capable of describing the main phenomena of such gyroscopic continua (Chen et al., 2007; Ding et al., 2012; Ding and Chen, 2010). In Fig. 4, the lower order natural frequencies are presented with increasing axial velocity. It is found that 4-term order truncation may yield good convergence in depicting the first two or four frequencies.

4. Eigenvalue analysis

By substituting

$$\begin{Bmatrix} \mathbf{Q} \\ \mathbf{P} \end{Bmatrix} = \begin{Bmatrix} \mathbf{C}_v \\ \mathbf{C}_z \end{Bmatrix} e^{\lambda t} \tag{17}$$

into (11) and subsequent numerical computation of the eigenproblem yield the eigenvalues λ and corresponding complex modes.

In the plots of Fig. 4, the real parts and the imaginary parts of the eigenvalues are plotted with varying axial moving speeds for fixed spinning velocities. The imaginary parts denote the natural frequencies of the system, while the real parts denote the corresponding damping-like quantity. Stability analysis implies the following three cases. Case 1: If the real parts of all the eigenvalues are zero or negative, the system is stable. Case 2: If the imaginary parts of all the eigenvalues are zero and one or more of the eigenvalues have positive real parts, the divergence occurs and causes the system to be unstable. Case 3: If one or more of the eigenvalues have both positive real part and nonzero imaginary part, the system will undergo flutter that leads to instability (Yang et al., 2011).

As presented in Fig. 4(a), the bifurcation series for mono-gyroscopic system of pure axial moving beam (Yang et al., 2011) is given. Without axial motion, v-direction and w-direction motions are not coupled and share the same dynamic characters due to symmetry. With emerging and increasing axial motion, the natural frequencies are lowered until the first order frequency vanishes, while the corresponding real part becomes positive. It is apparent that the divergence occurs at the critical axial moving speed $u = \pi$. The divergence-induced instability in the axially moving material is analogous to that of classical column buckling, where the axially moving speed has the interpretation of the compressive column load (Wickert, 1992).

With increasing further the axial moving speed to $u = 2\pi$, the system regains stability since all the real parts of the eigenvalues become zero and the formerly vanished frequency emerges again. If the axial moving speed increases further, the system may lose stability by flutter, beyond the critical values, $u = 6.4614$, where the two frequencies coalesce and at the same time the positive real part emerges. The flutter phenomenon of the axially moving material is termed as Païdoussis coupled-mode flutter, which is triggered by the frequency coalescence of the two sine basis functions (Païdoussis, 1998).

The series of bifurcations from stability to divergence-induced instability, and then from another stability to flutter-induced instability, is a typical phenomenon of axially moving material with both end supported, which has been widely discussed in the literature (Kim et al., 2003; Lin, 1997; Wickert and Mote, 1990; Yang et al., 2011).

If the spinning motion is considered, the vibrations in both v and w transverse directions are not isolated anymore: they are gyroscopically coupled. Every frequency bifurcates into two branches as presented in Fig. 6.

The most important distinct feature of the bi-gyroscopic system due to both axial and spinning motions, as compared to the mono-gyroscopic system of pure axial motion, is that the divergence phenomena can not be found for the bi-gyroscopic case. As presented in Fig. 5(b), the four natural frequencies are varying with axial velocity. The bi-gyroscopic system gives rise to flutter when the axial velocity reaches the critical value $u = \pi$, where the first two natural frequencies coalesce and one of the real parts of the eigenvalues becomes positive, which is a typical characteristic of coupled-mode flutter. With the increase of the axial velocity, the system regains stability as the lowest frequency branches into two and the real parts of the eigenvalues all become zero at $u = 2\pi$. If the axial velocity increases further, the first order frequency and the third order frequency coalesce and on the same point, $u = 6.4614$, and, furthermore, the second and fourth order frequencies also coalesce, which gives way to flutter since one of the eigenvalues emerges with positive real part. Hence, the bifurcation series of the bi-gyroscopic system along the axial velocity exhibit the behavior from stability to flutter-induced instability, and then from another stability to flutter-induced instability again. Recall that for the mono-gyroscopic system of the pure axial moving case, both divergence and flutter are found. The bifurcation series are listed in Table 2 for both the pure axial moving mono-gyroscopic and bi-gyroscopic systems.

It should be noted that the first and the second flutter phenomena of the bi-gyroscopic system are not the same. The first flutter is due to one pair of frequency coalescence which makes the first two modes coupled. However, the second flutter is due to two pairs of modes coupling at the same time. The stiffness coupling via matrix **D** plays a detuning role in the system: the stiffness coupling detunes the bi-gyroscopic system to let the two pairs of frequencies coalesce respectively, exactly at the same critical axial moving velocity. Evidently, the first coupled-mode flutter involves one repeated frequency and the second double-coupled-mode flutter involves two repeated frequencies. The double-coupled-

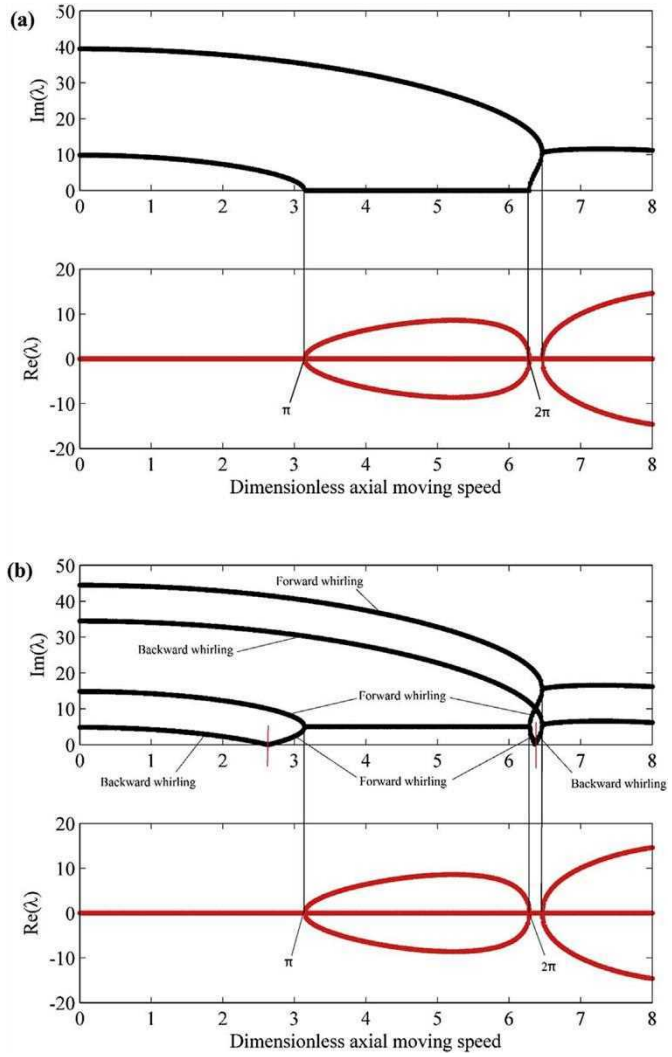

Fig. 5. Real and imaginary parts of eigenvalues vs. axial moving speed. (a) Dimensionless spinning speed $\Omega = 0$; (b) Dimensionless spinning speed $\Omega = 5$.

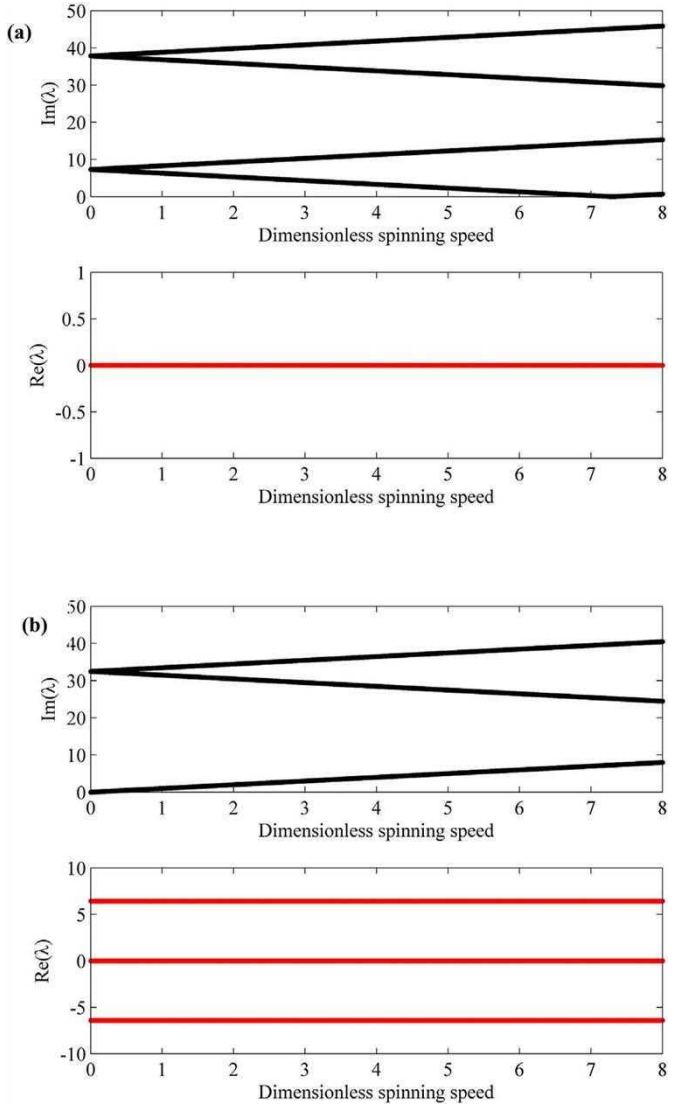

Fig. 6. Real and imaginary parts of eigenvalues vs. spinning speed. (a) Dimensionless axial moving speed $u = 2$; (b) Dimensionless axial moving speed $u = 4$.

mode flutter may accommodate more complicated dynamics in the further nonlinear analysis of such bi-gyroscopic systems.

Although the involvement of the spinning motion in the bifurcation along the axial motion changes the bifurcation series, the spinning motion does not change the critical values. Recall that there are three key couplings in the bi-gyroscopic system: (a) same direction coupling via axially moving velocity, (b) different direction coupling via spinning, and (c) the stiffness coupling via the product of both the axially moving and spinning velocities. Due to the contribution of the detuning effect of the stiffness coupling terms, the critical axial velocity always keeps the same value in the bifurcations regardless of the fact that the spinning velocities are given by different values. This can be verified by the condition analysis of repeated imaginary roots of the characteristic equations.

In Fig. 6, the eigenvalues with increasing spinning speed are presented for axial moving speeds $u = 2$ and 4, respectively. Every frequency bifurcates into two due to the fact that one backward whirling frequency and one forward whirling frequency exist for the spinning motion. For the axial moving speed $u = 4$ (Fig. 6(b)), only three frequencies are found, and the real part of one of the eigenvalues becomes positive. The reason for this phenomenon lies with the fact that $u = 4$ falls into the unstable regime as indicated in Fig. 5(b). Hence, the mono-gyroscopic system with pure spinning is stable in the whole region of the spinning velocity. On the other hand, the bi-gyroscopic system with both spinning and axial motion is also stable in the whole spinning speed range if the axial velocity is kept in the region of $0 \le u < \pi$ and $2\pi < u < 6.4614$. In other regions, the bi-gyroscopic system is always unstable.

Table 2
Bifurcation series for axial moving mono-gyroscopic and bi-gyroscopic systems.

	$0 \le u < \pi$	$\pi < u < 2\pi$	$2\pi < u < 6.4614$	$6.4614 < u$
Mono-gyroscopic system of the pure axial moving case	Stable	Divergence	Stable	Flutter (one pair repeated frequencies)
Bi-gyroscopic system	Stable	Flutter (one pair repeated frequencies)	Stable	Flutter (two pairs repeated frequencies)

In Fig. 6(a), the lowest frequency decreases with the spinning velocity and then increases after a turning point. The whirling direction of the first order modal motion will transfer from backward to forward. This phenomenon will be discussed further in Section 5.

To show the eigenvalue variations along the axial moving and spinning parameters, several illustrative three-dimensional plots are

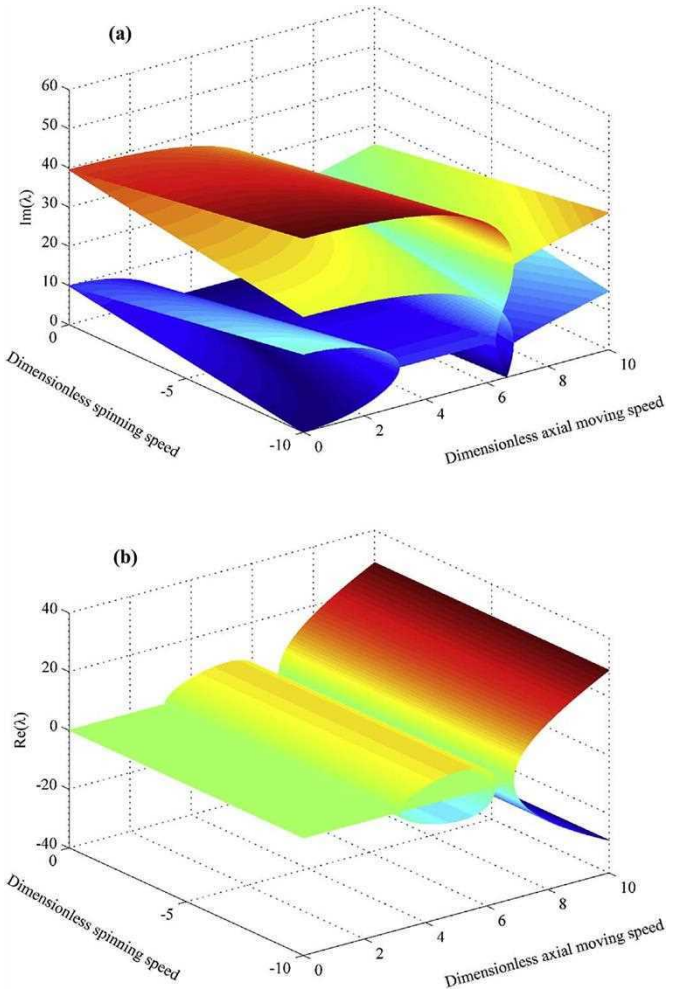

Fig. 7. 3D plots of varying eigenvalues. (a) Imaginary part; (b) Real part.

presented in Fig. 7. The occurrence of divergence and single-coupled-mode flutter of the mono-gyroscopic in the pure axially moving case is a particular case of the bi-gyroscopic system, which gives way to bifurcation of single-coupled-mode and double-coupled-mode flutters. The straight interception lines in parallel with the spinning speed axis imply that the critical values along the axial velocity are not affected by the spinning velocity values.

5. Complex modal motions

The modal motions in the stable regions can be described by the complex eigenvectors of the bi-gyroscopic system. Since both axial motion and spinning motion are involved, it is reasonable to locate combinations of whirling motions and traveling wave motions in the numerical display of the modal motions.

In both stable regions as presented in Fig. 5(b), $0 \leq u < \pi$ and $2\pi < u < 6.8693$, four modal motions corresponding to four natural frequencies can be obtained by (10). For the case of $u = 2$ and $\Omega = 5$, the four modal motions are plotted in Fig. 8. To clearly describe the whirling and traveling wave motions, the snapshots for different instances are presented to show the vibration contour of the system. In Fig. 8, it can be found the first mode and third modes are forward whirling motions, while the second and the fourth modes are backward whirling motions. On the other hand, the first and the second are leftward traveling wave, and the third and the fourth are right traveling wave (detailed discussions of the traveling wave of axially moving

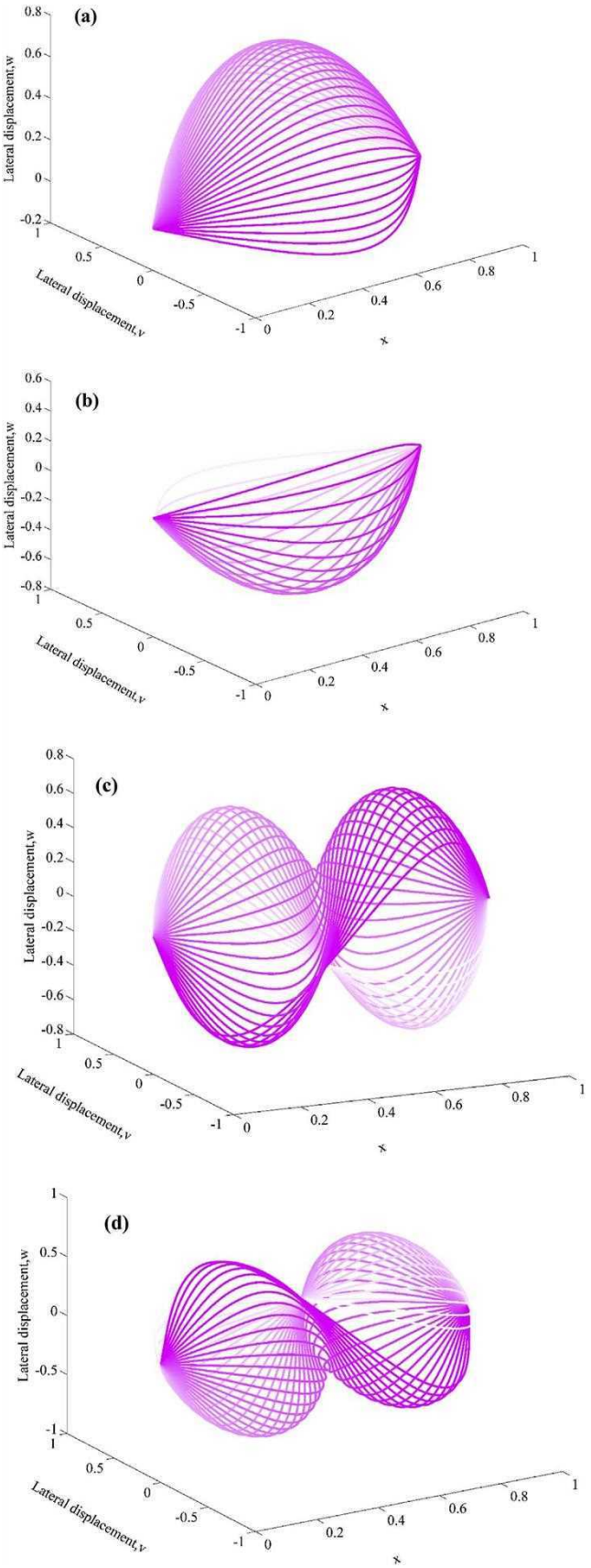

Fig. 8. Modal motions of in the subcritical region ($u = 2$ and $\Omega = 5$). (a) First mode; (b) Second mode; (c) Third mode; (d) Fourth mode.

material refer to (Yang et al., 2016)). However, if we increase the axial velocity, there exists a turning point, beyond which the first forward whirling mode becomes backward whirling. Such whirling direction turning makes possible the first and the second mode going to share the same value and leading to coupled-mode flutter on the critical point.

At the beginning of the second stable region, the first mode emerges as forward whirling, in the same way as just before it vanishes at the end of the first stable region. Beyond the second turning point, the whirling direction of the first mode is reversed. With further increase of axial velocity, the pair of forward whirlings coalesce and so do the backward whirlings, resulting in the double-coupled-mode flutter with two pairs of repeated frequencies. The matrix **D** has been found to guarantees the turning points will fall in the stable regions.

With the increase of the spinning velocity, the turning point in the first stable region is becoming farther away from the critical value π, tending to zero. The turning point in the second stable region is varying from 2π to the second flutter critical point.

6. Conclusions

In this study, the vibration of supported beam undergoing both axial motion and spinning has been investigated in detail. As an example of bi-gyroscopic systems, several interesting new phenomena have been found and some important conclusions have been derived based on the numerical display of the modal motions.

(1) The axial motion leads to the coupling of basis functions along the same transverse direction, while the spinning motion leads to the coupling of vibrations for different transverse directions. The axial motion causes a $\pi/2$ phase difference between any of the two adjacent general coordinates in the same direction, which gives rise to traveling waves modal in motions. The spinning motion causes a $\pi/2$ phase difference between the two transverse directions, which brings about the elliptic whirling modal motions.
(2) The stiffness coupling, in addition to the two types of gyroscopic couplings, have been found for the beam with both axial and spinning motions of bi-gyroscopic systems, while only gyroscopic couplings exist for the pure axial moving or pure spinning mono-gyroscopic cases.
(3) With the varying axial moving velocity, such a bi-gyroscopic system shows the bifurcation series from stability to flutter-induced instability, and from re-stability to flutter-induced instability again. Without the spinning motion, the mono-gyroscopic system for the pure axial moving case shows divergence for the first stable region. It is concluded that the critical points of the axial speed are not affected by the spinning velocities because of the detuning effect of the stiffness coupling.
(4) The first single-coupled-mode flutter is related to one pair of repeated frequencies and the second double-coupled-mode flutter is related to two pairs of repeated frequencies. The stiffness coupling detunes the bi-gyroscopic system to let the two pairs of frequencies coalesce respectively, exactly at the same critical axial moving velocity.
(5) In the first stable region, the first mode backward whirling motion becomes forward whirling when going through a turning point. In the second stable region, the first mode emerges as forward whirling, and then turns to backward whirling when going through the second turning point. The turning points are affected by the spinning velocity. Increasing spinning velocity makes the first turning point vary form π to zero in the first stable region and makes the second turning point varying from 2π to 6.4614 in the second stable region.

The interesting phenomena and important conclusions found in this study may provide a theoretical base for further investigations on the rich dynamics of bi-gyroscopic systems.

Acknowledgements

This work is supported in part by the National Natural Science Foundation of China (Project No. 11672007, 11672189, 11290152) and Beijing Natural Science Foundation (Project No. 3172003). Roderick Melnik was supported by the Natural Sciences and Engineering Research Council of Canada of Canada, the Canada Research Chair (CRC) program, and the Bizkaia Talent Grant under the Basque Government through the BERC 2014–2017 program, as well as Spanish Ministry of Economy and Competitiveness MINECO: BCAM Severo Ochoa excellence accreditation SEV-2013-0323.

References

Arvajeh, T., Ismail, F., 2006. Machining stability in high-speed drilling—Part 1: modeling vibration stability in bending. Int. J. Mach. Tool Manufact. 46, 1563–1572.
Chen, L.-Q., 2005. Analysis and control of transverse vibrations of axially moving strings. Appl. Mech. Rev. 58, 91–116.
Chen, S.H., Huang, J.L., Sze, K.Y., 2007. Multidimensional Lindstedt–Poincaré method for nonlinear vibration of axially moving beams. J. Sound Vib. 306, 1–11.
Cooley, C.G., Parker, R.G., 2014. Vibration of high-speed rotating rings coupled to space-fixed stiffnesses. J. Sound Vib. 333, 2631–2648.
Ding, H., Chen, L.-Q., Yang, S.-P., 2012. Convergence of Galerkin truncation for dynamic response of finite beams on nonlinear foundations under a moving load. J. Sound Vib. 331, 2426–2442.
Ding, H., Chen, L.Q., 2010. Galerkin methods for natural frequencies of high-speed axially moving beams. J. Sound Vib. 329, 3484–3494.
Fang, J.C., Ren, Y., Fan, Y.H., 2014. Nutation and precession stability criterion of magnetically suspended rigid rotors with gyroscopic effects based on positive and negative frequency characteristics. IEEE Trans. Ind. Electron. 61, 2003–2014.
Genta, G., 2005. Dynamics of Rotating Systems. Springer Science + Business Media, Inc., New York.
Genta, G., Silvagni, M., 2013. On centrifugal softening in finite element method rotordynamics. J. Appl. Mech. 81, 011001.
Kim, J., Cho, J., Lee, U., Park, S., 2003. Modal spectral element formulation for axially moving plates subjected to in-plane axial tension. Comput. Struct. 81, 2011–2020.
Kim, W., Chung, J., 2002. Free non-linear vibration of a rotating thin ring with the in-plane and out-of-plane motions. J. Sound Vib. 258, 167–178.
Lin, C.C., 1997. Stability and vibration characteristics of axially moving plates. Int. J. Solid Struct. 34, 3179–3190.
Öz, H.R., Pakdemirli, M., 1999. Vibrations of an axially moving beam with time-dependent velocity. J. Sound Vib. 227, 239–257.
Païdoussis, M.P., 1998. Fluid-structure Interactions: Slender Structures and Axial Flow, vol 1 Elsevier Academic Press, London.
Parker, R.G., Sathe, P.J., 1999a. Exact solutions for the free and forced vibration of a rotating disk-spindle system. J. Sound Vib. 223, 445–465.
Parker, R.G., Sathe, P.J., 1999b. Free vibration and stability of a spinning disk-spindle system. J. Vib. Acoust. 121, 391–396.
Parker, R.P., 1998. On the eigenvalues and critical speed stability of gyroscopic continua. J Appl Mech-T Asme 65, 134–140.
Pei, Y.-C., Sun, Y.-H., Wang, J.-X., 2013. Dynamics of rotating conveying mud drill string subjected to torque and longitudinal thrust. Meccanica 48, 2189–2201.
Pellicano, F., Vestroni, F., 2000. Nonlinear dynamics and bifurcations of an axially moving beam. J. Vib. Acoust. 122, 21–30.
Rincon, D.M., Ulsoy, A.G., 1995. Complex geometry, rotary inertia and gyroscopic moment effects on drill vibrations. J. Sound Vib. 188, 701–715.
Wickert, J.A., 1992. Non-linear vibration of a traveling tensioned beam. Int. J. Non Lin. Mech. 27, 503–517.
Wickert, J.A., Mote, C.D., 1989. On the energetics of axially moving continua. J. Acoust. Soc. Am. 85, 1365–1368.
Wickert, J.A., Mote, C.D., 1990. Classical vibration analysis of axially moving continua. J Appl Mech-T Asme 57, 738–744.
Wu, J.S., Lin, F.T., Shaw, H.J., 2014. Analytical solution for whirling speeds and mode shapes of a distributed-mass shaft with arbitrary rigid disks. J Appl Mech-T Asme 81.
Yang, X.D., Chen, L.Q., Zu, J.W., 2011. Vibrations and stability of an axially moving rectangular composite plate. J Appl Mech-T Asme 78, 011018.
Yang, X.D., Yang, S., Qian, Y.J., Zhang, W., Melnik, R.V.N., 2016. Modal analysis of the gyroscopic continua: comparison of continuous and discretized models. J Appl Mech-T Asme 83, 084502.
Yu, D.L., Paidoussis, M.P., Shen, H.J., Wang, L., 2014. Dynamic stability of periodic pipes conveying fluid. J Appl Mech-T Asme 81, 011008.
Zhang, Q., Miska, S., 2005. Effects of flow–pipe interaction on drill pipe buckling and dynamics. J. Pressure Vessel Technol. 127, 129.